

VASCULAR IMAGING

New techniques for the reconstruction of complex vascular anatomies from MRI images

DAVID H. FRAKES,^{1,2,*} MARK J. T. SMITH,³ JAMES PARKS,⁴ SHIVA SHARMA,⁵ MARK FOGEL,⁶
and AJIT P. YOGANATHAN¹

¹Wallace H. Coulter Department of Biomedical Engineering, Georgia Institute of Technology, Atlanta, Georgia, USA

²4-D Imaging, Inc., Atlanta, Georgia, USA

³School of Electrical and Computer Engineering, Purdue University, West Lafayette, Indiana, USA

⁴Sibley Heart Center, Children's Healthcare of Atlanta, Atlanta, Georgia, USA

⁵Atlanta Cardiology Associates, Atlanta, Georgia, USA

⁶Children's Hospital of Philadelphia, Philadelphia, Pennsylvania, USA

The accurate representation of two-dimensional images in three dimensions has become important for many medical imaging applications and for cardiac magnetic resonance imaging (MRI) in particular. Reconstruction methods applied after data acquisition can produce three-dimensional information from two-dimensional data and make applications such as surgical planning more effective. Current reconstruction techniques usually demand contrast agents, and can suffer due to poor segmentation and sampling constraints that cause surface irregularities and distort dimensions. The novel technique presented here for anatomical modeling uses adaptive control grid interpolation (ACGI) to approximate data not captured by scanning, and a progressive shape-element segmentation technique to complete reconstruction. Quantitative validations conducted on models of pediatric cardiac malformations have confirmed the theoretical advantages of this technique, and that higher quality is achieved than with competing methods based on geometric parameters. Vascular diameters from reconstructions showed errors of less than 1% for a known geometry as compared to over 9% for competing methods. Qualitatively, models produced with the new methodology displayed substantial improvement over alternatives. Approximately 50 rare cardiac structures, including surgically altered Fontan and atypical aortic anatomies, have been reconstructed. All data used to create these reconstructions were acquired using standard pulse sequences and without contrast agents. Benefits of the new technique are particularly evident when complex vascular configurations complicate reconstruction. The proposed methodology enables a powerful tool allowing physicians to analyze and manipulate highly accurate and clearly presented vascular structures in an interactive medium.

Key Words: Reconstruction; Segmentation; Surgical planning; Vascular; Fontan

1. Introduction

The advent of magnetic resonance imaging (MRI) has equipped clinicians with valuable technology for the non-invasive analysis of anatomy and physiology. In one of its most common forms, two-dimensional (2D) imaging, MRI acquires parallel planar samples from a three-dimensional (3D) data source. These samples can later be reconstructed to model specific 3D structures from the original imaging target. Cardiovascular medicine is one area that has been advanced by MRI, and now relies heavily on both the modality itself and reconstruction to enable applications such as surgical planning.

Like all imaging modalities, MRI has its shortcomings, one of which is the tradeoff between spatial resolution and

signal-to-noise ratio (SNR). Averaging greater numbers of signals and performing oversampling can offer benefits, but do nothing to change this fundamental compromise. For many MR applications based on 2D imaging, in-plane resolution is deemed more important and out-of-plane resolution is sacrificed in order to maintain SNR. Under other circumstances, an image stack composed of isotropic voxels is more desirable, and is acquired at the expense of in-plane resolution. Both of these cases present problems that relate to the interpolation and segmentation components of reconstruction scenarios. In the first case, data sets are commonly gathered with in-plane pixel dimensions of less than 1 mm but with slice thicknesses of 3 to 5 mm, which becomes problematic for 3D reconstruction. To counteract this, interpolation is used to approximate information lost to undersampling. Examples of raw and interpolated data sets are offered in Fig. 1. Like all interpolation problems, the quality of approximated data in the MR case is a function of the methods used and can vary significantly among techniques. The data in Fig. 1(b) were interpolated with the novel approach to be presented here.

Received 18 June 2004; accepted 11 November 2004.

*Address correspondence to David H. Frakes, 4-D Imaging Inc., 75 Fifth St., Suite 331, Atlanta, GA 30308, USA; Fax: (404) 385-4153; E-mail: dave@bme.gatech.edu

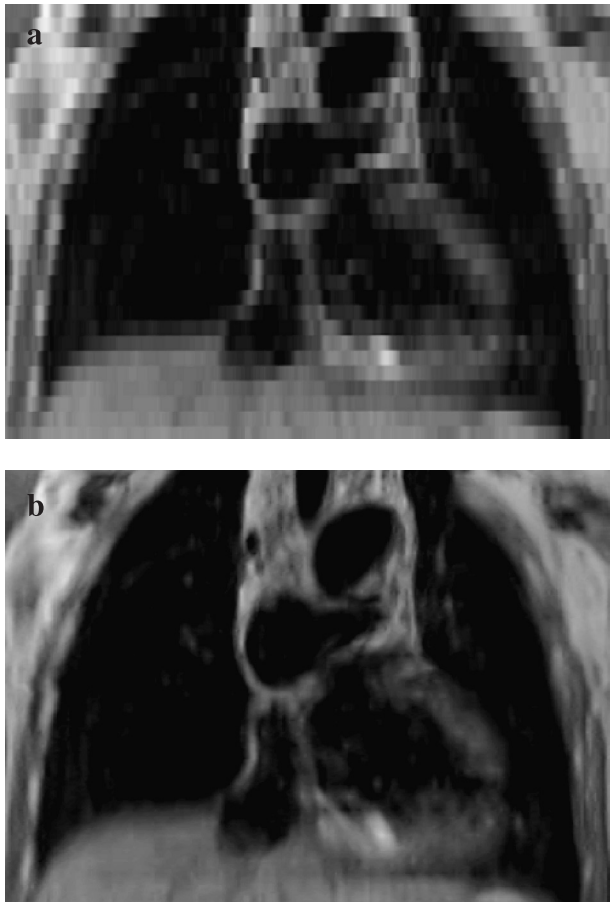


Figure 1. Example of raw (a) and ACGI enhanced (b) cardiac MR data sets. ACGI enhancement produces MR data sets that exhibit similar resolution to CT.

When isotropic voxels are acquired, the manifestations of undersampling and averaging may be more apparent in the in-plane data. Partial volume effects cause the boundaries of structures like blood vessels to be poorly defined, rendering many basic segmentation strategies ineffective. Under these circumstances, more creative approaches are required to segment accurately. In practice, all 2D MR data sets exhibit, to some extent, manifestations of the spatial resolution/SNR tradeoff. The problem of reconstructing these data has been addressed in the past, but there remains a great deal of room for improvement (1–17). Difficult scenarios like those that involve complex cardiac vasculatures pose even further challenges and require robust solutions (12, 13).

The new methodology presented here approaches the reconstruction problem from a different perspective and was designed for application to tortuous small-scale vascular structures. Current practice often calls for the use of specialized pulse sequences and contrast agents to facilitate reconstruction, but all data presented here were acquired with standard pulse sequences and without any contrast agents. This technique allows more to be done with routine data at a lesser cost. The novel interpolation and segmentation

strategies that define the technique create a tool that performs with higher quality than other state-of-the-art approaches, and is capable of addressing reconstruction problems that those methods cannot.

2. Methods

The interpolation portion of the reconstruction methodology presented here was inspired by techniques originally designed for motion estimation in nonmedical video sequences. In this implementation, motion estimation is accomplished with a form of adaptive control grid interpolation (ACGI). Addressing the problem from this perspective is new and differs significantly from other reconstruction protocols that have been proposed. The primary features that distinguish this new technique from others are the order and manners in which data interpolation and segmentation are performed.

2.1. Order of events

In most traditional approaches, segmentation, or the isolation of particular regions of interest within slices of a medical image set, is performed prior to reconstruction. Simply put, features of an anatomical structure are first identified within each slice and these isolated regions are then connected via some interpolation function. This order of events is problematic in that any errors introduced during the segmentation process propagate into the reconstruction. As no segmentation scheme is perfect in practice, errors will occur regardless of the methodology employed. For this reason it is advantageous to perform segmentation last and ensure that segmentation errors are isolated. This is the order of events followed within the new reconstruction framework presented here: ACGI is first used to interpolate data, which are then segmented via shape element segmentation. The down side of these mechanics is that there are a greater number of images to be segmented. However, given the availability of a robust and efficient automated segmentation algorithm, the ill effects of segmenting a larger number of images are minimal.

2.2. Data interpolation

Another component of the new methodology that distinguishes it from competing techniques is the mechanism by which data interpolation is accomplished. As has been previously discussed, the majority of currently popular approaches segment first and then connect features of an anatomical structure from different slices via an interpolation function. This procedure is flawed in that only the isolated regions from respective images are used to approximate missing data between the acquired slices. In any interpolation problem it is fundamentally advantageous to use all available information for the approximation of intermediate data. The approach presented here does exactly that.

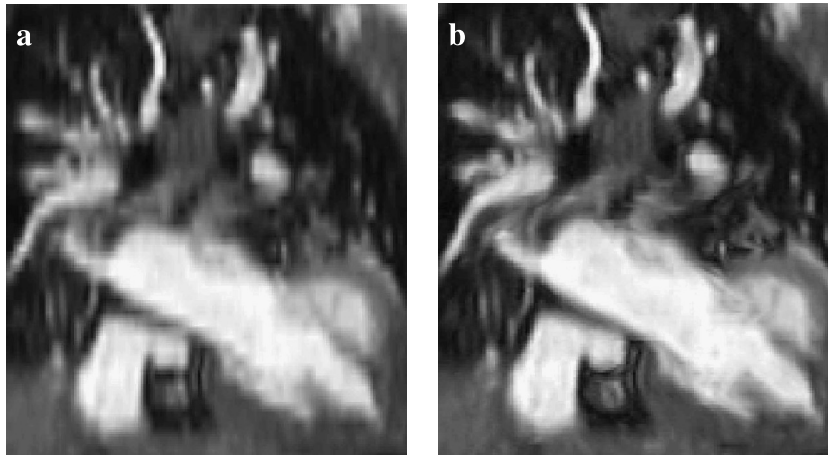


Figure 2. Coronal MPR views of an axially acquired MR data set enhanced with (a) trilinear interpolation and (b) ACGI. The former strategy is popular in current MPR applications.

Data interpolation is accomplished via ACGI, whereby motion estimation is used to determine vectors that link the features of anatomical structures found in different slices. By interpolating along these vectors it is possible to reconstruct entire planes of data between the acquired slices. This process results in an enhanced data set that displays significantly greater spatial resolution in the out-of-plane direction, as compared to the original data. Like all interpolation strategies, the ACGI technique approximates unknown data points based on known ones. As such, circumstances do arise when interpolated data deviate from reality. However, because interpolation is carried out between points from correlated structures, data approximated via ACGI is more likely to be realistic than data approximated based on traditional nondirectional approaches.

Evidence in support of this, and a more detailed account of the mathematics behind ACGI, can be found in a recent *IEEE Transactions on Biomedical Engineering* article (18).

Here the entire data set is reconstructed prior to any segmentation operations. MR data sets enhanced with this technique resemble CT data in terms of quality. One such data

set is shown in multi-planar reconstruction format in Fig. 1, where a stack of axially acquired images is being viewed from the coronal perspective. In addition to presenting a substantial improvement over raw data, ACGI enhancement compares favorably with single-image-based interpolation schemes that are popular in current MPR interfaces. An example of a trilinearly interpolated frame, and the corresponding ACGI-enhanced version, are shown in Fig. 2. Unlike single-image-based interpolation strategies, ACGI reconstructs entire intermediate frames and produces a data set consisting of isotropic voxels throughout. Accordingly, the visualization of any plane or perspective, or combination thereof, is possible with consistent high quality. Figure 3 shows an axial-sagittal combination visualization in (a) and an example of an oblique plane in (b).

2.3. Segmentation

The way in which segmentation is performed in this new methodology differs significantly from traditional approaches

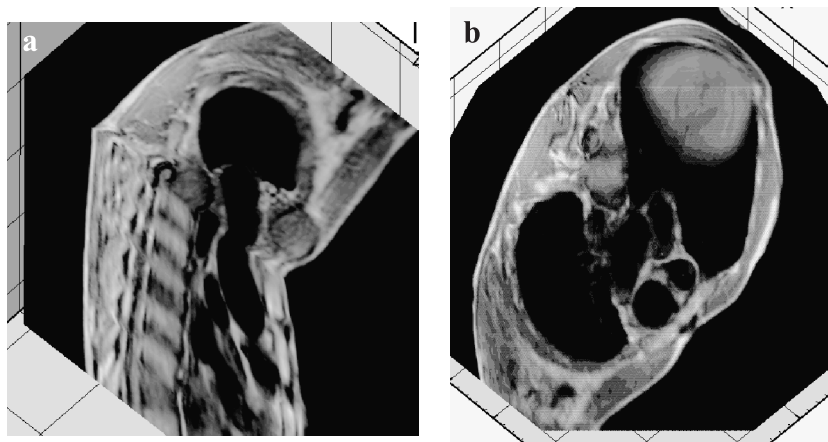


Figure 3. Visualizations of (a) an axial/sagittal combination and (b) an arbitrarily selected oblique plane from an ACGI-enhanced data set.

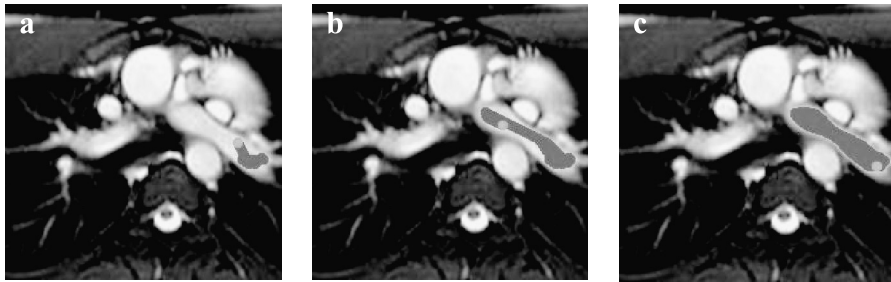


Figure 4. Frames from segmentation process after (a) five iterations, (b) 15 iterations, and (c) at completion. The light intensity ball represents the current location of the segmentation particle while the darker gray region represents the area that has been covered by the path of the particle.

as well. Fundamental techniques such as thresholding, edge-detection, various forms of region growing, and manual feature identification remain popular in today's medical image processing software packages. Problems that confront such techniques arise from the aforementioned relationship between spatial resolution and SNR. Thin slice thicknesses can be used to avoid undersampling, but compromise SNR. Alternatively, SNR can be increased by using larger pixel dimensions, but in-plane resolution is sacrificed. Poorly defined anatomical boundaries are one manifestation of both versions of this unavoidable tradeoff. At such locations intensity and gradient-based thresholding and edge-detection approaches will be ineffective in completely defining an area of interest. To address this problem the assumption is made that the regions where boundaries are incomplete are localized, and that simple traditional techniques like thresholding and edge detection can be successful in defining much of a region border.

In the new approach, shape element segmentation, the incompletely identified borders are used as a scaffold within which areas of interest are constructed. Because the border gaps are of limited size when parameters are chosen appropriately, they prohibit a sufficiently large particle from escaping the interior of the structure. One can consider the classical leaky container analogy to illustrate this assumption. If a leaky container is filled with water, the water seeps out, leaving the container empty. If, however, larger particles

are used for filling, grains of sand perhaps, the container remains full.

This simple realization is the fundamental principle behind shape element segmentation. Using segmentation particles, or shape elements, larger than border gaps, it is possible to define the region of interest well. This automated process is illustrated in Fig. 4 where the shape element bounces within the intensity-defined scaffold an effectively infinite number of times to fill the entire area of interest. The use of any shape element larger than an individual pixel does effectively low pass filter the vessel border, so it is advantageous to use as small a shape element as possible in order to retain detail in the extracted vascular boundary. In practice, a spherical shape element with a radius of 2.5 pixels is used preferentially, as it is the smallest element of that configuration that describes a spherical profile reasonably well. When this element proves too small and leakage is detected, the element size is incremented and segmentation is repeated at local regions surrounding the leakage site. It is also noteworthy that in execution this procedure is performed as a special case of region growing to avoid redundant retracing of the vessel interior. Results have indicated that using a shape element, as opposed to a single pixel, does not sacrifice segmentation accuracy at the hands of feasibility given that data sets are of sufficient resolution. All data sets examined here met this criterion with pixel dimensions in the submillimeter range. Even in cases where highly stenotic vessel features were

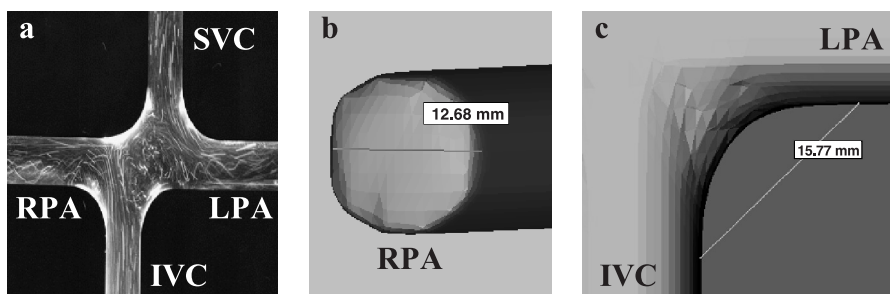


Figure 5. In vitro glass TCPC model used for reconstruction (a), and illustrations of geometric parameters used to validate the ACGI reconstruction technique: (b) pulmonary artery diameter and (c) connection geometry radius of curvature.

Table 1. Quantitative results from in vitro reconstruction validation

	Original	ACGI	Spline	Linear
PA Diameter (mm)	13.59	13.72	13.69	12.36
% Error	N/A	0.96%	0.74%	9.05%
Radius of curvature (mm)	7.92	8.06	9.03	7.46
% Error	N/A	1.77%	14.02%	5.81%

present, the shape element technique performed well as reported in another recent study (19).

3. Results

This application was developed in the context of treating pediatric cardiac malformations. More specifically, analysis of the Fontan geometry, surgically created to treat single ventricle congenital heart defects, was focused upon. Accordingly, the in vitro models used to validate the ACGI reconstruction methodology were designed to mimic the anatomical district modified by the Fontan operation. One such model, of a total cavopulmonary connection (TCPC), is shown in Fig. 5(a). The in vivo examples of ACGI reconstruction that are shown later in this section are from Fontan cases and pediatric patients with other cardiovascular disorders.

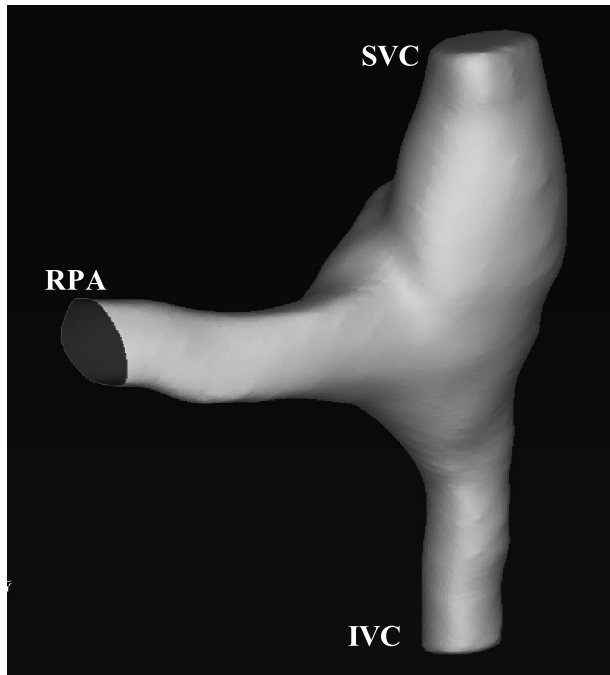


Figure 6. Right sagittal view of a total cavopulmonary connection from a dextracardiac patient. This Fontan geometry is atypical in that a large superior vena cava and connection region are observed in comparison to the much smaller inferior vena cava.

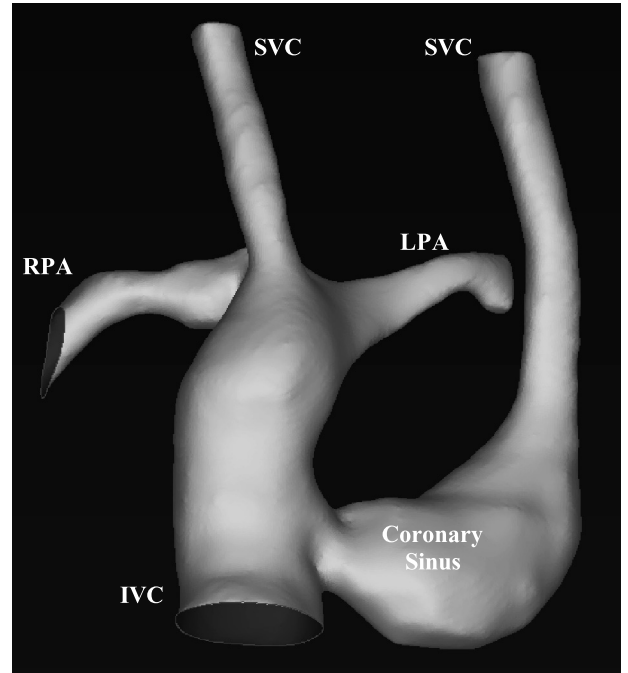


Figure 7. Coronal view of a rare bilateral superior vena cava Fontan configuration with one superior vena cava connecting to the inferior vena cava via a bulbous coronary sinus.

3.1. In vitro validation

MR scans of the Fontan model were conducted and the acquired data were reconstructed using the ACGI methodology and two other competing techniques: morphology-based linear interpolation and contour-based cubic spline interpolation (6,13). These approaches have been used to address

Table 2. Example parameters from MR data acquisition

Parameter	Setting
Pulse sequence	True fisp
TR	166 ms
TE	1.59 ms
FOV	150 mm
Slice thickness	3 mm
Distance factor	0
Matrix	100 × 128
NEX	3
Segments	29
Trigger delay	334 ms
Number of slices	45
Rectangular FOV	80%
Acquisition window	500
Flip angle	90 degrees
Echo spacing	3.2 ms
Partial phase fourier	0
Bandwidth	1220 hz/px

the reconstruction problem frequently in recent literature (4, 8, 11, 20, 21). Reconstruction results were compared based on two geometric parameters of the Fontan model known to contribute significantly to fluid dynamics, connection geometry radius of curvature, and pulmonary artery diameter. Specifically, these parameters from the reconstructed models were compared to the same parameters from the originally scanned model. These two characteristics are highlighted in Fig. 5(b) and 5(c).

Connection geometry radius of curvature measurements were taken for each of the four transition regions and averaged. Pulmonary artery diameter measurements were taken at each of the model outlets and these numbers were averaged as well. The results of the validation affirm that ACGI reconstruction performs with higher quality than either

competing method. The error values associated with each reconstruction are given in Table 1. Repeatability was established by performing reconstruction 100 times for each case, and individual trial results were averaged to yield the results in Table 1. In addition to the measures listed in Table 1, the ACGI-reconstructed model varied from the original by less than 4% in terms of pulmonary artery diameter at any cross-section, and by less than 6% in terms of total TCPC model volume.

3.2. *In vivo* results

Following validation, approximately 50 cardiovascular structures were reconstructed. Several examples of these reconstructions are shown in Figs. 6–8. These visualizations are of

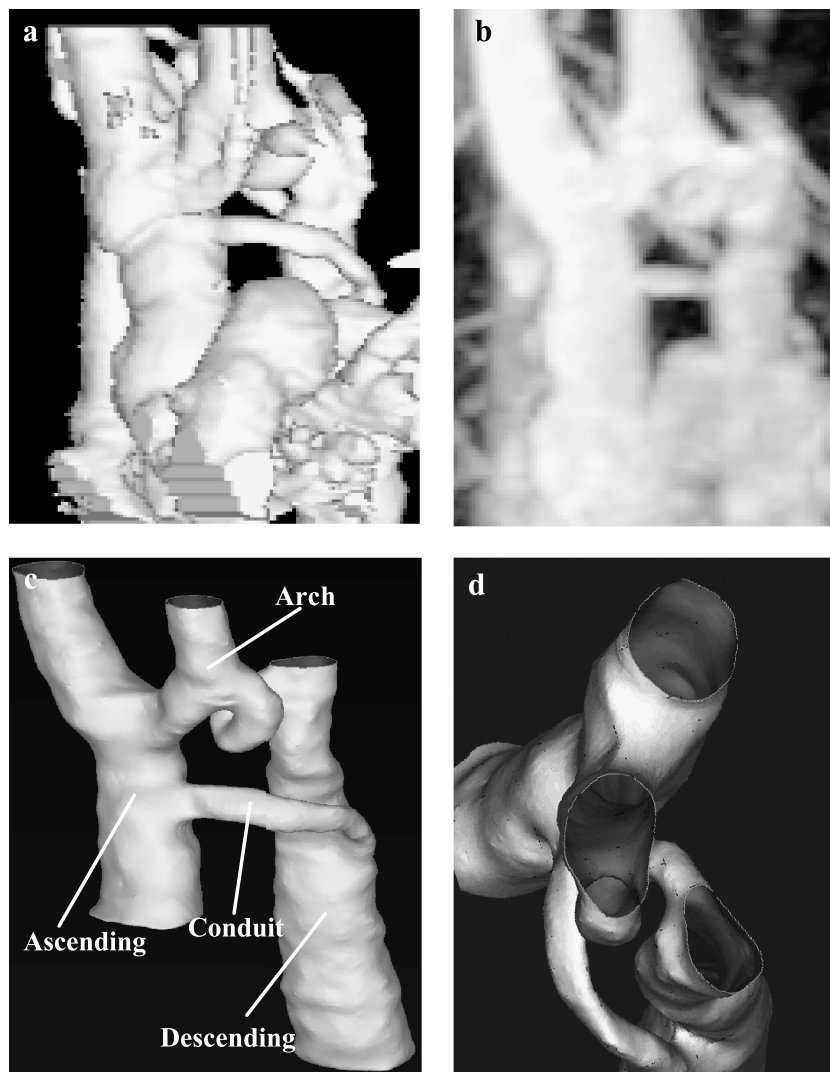


Figure 8. Shaded surface representation (a), maximum intensity projection model (b), and ACGI reconstruction (c) and (d) of a rare corkscrew aortic configuration. Both (a) and (b), taken directly from a major manufacturer's reconstruction package, were produced from data acquired using gadolinium, while (c) and (d) were created from images acquired with a standard pulse sequence and without any contrast agents. In (d) a superior perspective cutaway highlights the visualization versatility inherent to models created with the new methodology.

stereo lithography (STL) files created from the reconstructed data sets with in-house code written in Matlab (22). The files are visualized in Magics Communicator, a stand-alone STL viewer (23). In some cases, reconstructions produced by major MR hardware manufacturer packages were also available. One comparison of a maximum intensity projection and a shaded surface representation to an ACGI reconstruction is provided in Fig. 8. All of the ACGI reconstructions presented here were created from data acquired with standard pulse sequences and without contrast agents. More specifically, either True FISP (Siemens, New York, NY) or Fiesta (GE, Waukesha, WI) sequences were used in all cases. An example set of scan parameters are provided in Table 2 for reference.

In Fig. 8 the corkscrew aorta reconstructions reveal the shortcomings of two popular approaches. The maximum intensity projection clearly suffers from poor resolution and a lack of segmentation, while the shaded surface representation suffers from poor segmentation as well and also the effects of undersampling where jagged edges are observed. It is noteworthy that both (a) and (b) were created using data from a gadolinium-enhanced magnetic resonance angiography (MRA) scan, while the reconstruction in (c) and (d) was produced from data acquired with a standard pulse sequence and without the use of any contrast agents.

In addition to the improvements that are clear from a static image, the combined use of ACGI and shape element segmentation produces more complete information that can be viewed and manipulated interactively with consistent high quality. This includes simple perspective manipulations as well as more advanced visual operations. In Fig. 8(d) a superior perspective cutaway is showcased, allowing focused analysis and accurate dimensional quantification of the corkscrew region.

4. Discussion

The concept of data reconstruction is not new and many techniques have been proposed for the transition of two-dimensionally sampled data into three dimensions. The majority of these techniques suffer due to segmentation and resolution problems. The approach taken in this work addresses both concerns. Adaptive control grid interpolation is used to enhance out-of-plane spatial resolution in acquired data sets and shape-element segmentation is used to isolate regions of interest. In validations, the combination of these techniques performed with superior quality in comparison to other state-of-the-art methods from recent literature. Additionally, the results presented here compared favorably from a qualitative standpoint to examples produced by major manufacturer MPR and reconstruction packages.

The primary thrust of this paper is to demonstrate a reconstruction methodology that represents a fundamental technical advancement. However, there are a number of

noteworthy implications in terms of practicality as well. All of the reconstructed morphologies presented, except those included as counterexamples, were created based on data acquired with True FISP (Siemens, New York, NY) and Fiesta (GE, Waukesha, WI) pulse sequences. These sequences can be executed more quickly than alternatives, and do not demand contrast agents or the clinical assistants required to administer them. Accordingly, the scans used for reconstruction here can be performed in less time, with less risk, and at a lower cost. Furthermore, since the aforementioned pulse sequences capture the anatomy within each slice at various points over the course of the heart cycle, reconstruction via the proposed means can create dynamic time-varying morphological models that pulse with blood flow. MRA, in contrast, provides only a single static representation of a vascular structure at a lone point in time.

Though the components defining the methodology presented here are most powerful when combined, each offers benefits on an individual basis as well. Data sets interpolated with ACGI provide significantly higher quality for MPR applications in comparison to bilinear and bicubic interpolation kernels. Several additional characteristics of shape element segmentation are also noteworthy, especially in the context of vascular imaging. First, the “inside out” approach allows the characterization of the interior of the vessel wall, which is where the interesting and significant structural features are located with respect to blood flow. Next, the approach eliminates the need to strip away layers of material corresponding to contiguous structures outside of the vessel that appear connected based on intensity. This is a feature of simpler region growing and watershed strategies as well, but the shape element development improves on these by prohibiting the segmented region from jumping out of the vessel to areas of similar intensity.

Complex three-dimensional anatomies like those found in patients with atypical cardiac disorders are often extremely intricate and complicate the fundamental problem of reconstruction. Modeling such anatomies based on two-dimensional image samples has proven problematic for traditional means. However, these cases are no less important than the simpler ones, and must be addressed successfully. The combination of ACGI and shape-element segmentation creates a more robust solution to the problems posed by complex morphologies, and establishes a valuable anatomic modeling tool for vascular surgical planning and other cardiac MRI applications.

Acknowledgments

This work was supported by a grant from the National Institutes of Health: NHLBI (R01HL67622). The Children’s Hospital of Philadelphia, Egleston Children’s Hospital, Emory University, and the University of North Carolina at Chapel Hill have also contributed significantly to this research.

References

1. Spicer C, Taylor C. Simulation-based medical planning for cardiovascular disease: visualization system foundations. *Comput Aided Surg* 2000; 2:82–89.
2. Denney T, McVeigh E. Model-free reconstruction of three-dimensional myocardial strain from planar tagged MR images. *J Magn Reson Imaging* 1997; 7:246–249.
3. Wang K, Dutton R, Taylor C. Improving geometric model construction for blood flow modeling. *IEEE Eng Med Biol Mag* 1999; 6:33–39.
4. Saber N, Gosman A, Wood N, Kilner P, Charrier C, Firmin D. Computational flow modeling of the left ventricle based on in vivo MRI data: initial experience. *Ann Biomed Eng* 2001; 29:275–283.
5. Taylor C, Hughes T, Zarins C. Finite element modeling of three-dimensional pulsatile flow in the abdominal aorta: relevance to atherosclerosis. *Ann Biomed Eng* 1998; 6:975–987.
6. Moore C, O'dell W, McVeigh E, Zerhouni E. Calculation of three-dimensional left ventricular strains from biplanar tagged MR images. *J Magn Reson Imaging* 1992; 2:165–175.
7. He J, Zha H, Shi Q. Reconstruction of surfaces from medical slices using a multi-scale strategy. *Proceedings IEEE International Conference on Systems, Man, and Cybernetics*. Vol. 1. 2000:1993–1998.
8. Wen-Xue Y, Li-Min L, Yao F, Hua-Zhong S, Giband B. Intermediate contour interpolation for computed atlas surface reconstruction of the 3-D human brain. *Acta Electron Sin* 2000; 28:52–54.
9. Morita S, Takata H. Surface generation of interpolative images by determining elasticity of active contour model. *Syst Comput Jpn* 1999; 30:493–500.
10. Chen S, Lin W, Liang C, Chen C. Improvement on dynamic elastic interpolation technique for reconstructing 3-D objects from serial cross sections. *IEEE Trans Med Imag* 1990; 9:71–83.
11. Lee T, Wang W. Morphology-based three-dimensional interpolation. *IEEE Trans Med Imag* 2000; 19:711–721.
12. Higgins W, Morice C, Ritman E. Shape-based interpolation of tree-like structures in three-dimensional images. *IEEE Trans Med Imag* 1993; 12:439–450.
13. Treede G, Prager R, Gee A, Berman L. Surface interpolation from sparse cross sections using region correspondence. *IEEE Trans Med Imag* 2000; 19:1106–1114.
14. Grevera G, Udupa J. Shape-based interpolation of multidimensional grey-level images. *IEEE Trans Med Imag* 1996; 15:881–892.
15. Raya S, Udupa J. Surface shape-based interpolation of multidimensional objects. *IEEE Trans Med Imag* 1990; 9:32–42.
16. Grevera G, Udupa J. An objective comparison of 3-D image interpolation methods. *IEEE Trans Med Imag* 1998; 17:642–652.
17. Bors A, Kechagias L, Pitas I. Binary morphological shape-based interpolation applied to 3-D tooth reconstruction. *IEEE Trans Med Imag* 2002; 21:100–108.
18. Frakes D, Conrad C, Healy T, Monaco J, Smith M, Fogel M, Sharma S, Yoganathan A. Application of an adaptive control grid interpolation technique to morphological vascular reconstruction. *IEEE Trans Biomed Eng* 2003; 50:197–206.
19. Pekkkan stenosis.
20. Szeliski R, Shum H. Motion estimation with quadtree splines. *IEEE Trans Pattern Anal Mach Intell* 1996; 18:1199–1210.
21. Werahera P, Miller G, Taylor G, Brubaker T, Daneshgari F, Crawford E. A 3-D reconstruction algorithm for interpolation and extrapolation of planar cross sectional data. *IEEE Trans Med Imag* 1995; 14:765–771.
22. Matlab (Computer Program). Release 13. Mathworks: Natick, MA, 2003.
23. Magics Communicator (Computer Program). Release 2.30. Materialise: Ann Arbor, MI, 2003.